CHAPTER 6 Coalescence Avalanches in 2D Emulsions: a stochastic framework

6.1 PRELUDE

Coalescence is a process by which individual entities combine to form one large entity. In droplet microfluidics, the drops which are dispersed in the continuous fluid inside a channel can approach each other and merge to form larger drops. The two-drop coalescence problem is a non-linear and multi-scale problem that spans across several orders of magnitude in the length and time scales[88,128–130]. When two drops approach each other they displace the continuous phase between them. As a result of this thin film drainage problem, large velocity gradients are produced, which in turn generate large pressures between the drops that slows down their approach. This is similar to the interaction that the drops experience in the diverging converging microchannels, discussed in earlier chapters, that results in layering. As the drops continue to approach each other, the lubrication pressure fields also result in the deformation of the interface which results in complex interface configurations, like pimple, wimple and dimple, which complicate the drainage profiles. When the thickness of the film goes down to a few nanometers, van der Waal's forces become important and can destabilize the film allowing the drop interfaces to meet, initiating coalescence[88]. Theoretical and experimental investigations on the two-drop coalescence problem have been carried out in an attempt to understand the dynamics and stability of an emulsion[64,131–134]. From sophisticated force measurements and high fidelity mathematical models[135] to time and space resolved microfluidic experiments[8,14,46,65,136–139] have been performed, to explore the underlying mechanisms of coalescence.

Designing microchannels that accomplish a task would involve the manipulation of these drops inside channels where they can be subject to different conditions. Depending on the application at hand, one may or may not prefer coalescence of drops as they are manipulated in microchannels. Consider the case where one intends to carry out a reaction between two reactants A and B. Reactants A and B can be isolated into different drops and subject to several processes before allowing them to react. Reaction can be initiated by allowing the drops to coalescence (preference for coalescence). By controlling the proportion in which the different drops are coalesced, the amount of A and B in the resultant drop can be manipulated to control the rate of the reaction. By carefully manipulating the surfactant concentration on the interface of the drops, Mazutis et al showed that it is possible to restrict the amount of coalescence events that a drop can undergo[138]. Here is another example where coalescence is not preferred during device operation. Consider the working of a droplet-incubator, a microfluidic device that holds drops for a stipulated amount of time which may range from minutes to hours[23,24]. A typical incubation device is a 2D or a 3D microchannel that houses a large number of drops, tightly packed, moving in the channel at small velocities. A successful incubation process will require the drop assembly to be stable and free of coalescence under operating conditions (no preference for coalescence). Hence, from a design perspective it becomes necessary to understand the dynamics of coalescence, as a function of the complex self-organization of drops and geometry of the packing. Experimental evidence shows that coalescence in an ensemble of drops can result in very different behaviors: Migler showed that as shear rate was decreased, drops organized and coalesced to form liquid strings[140]; Bremond and co-workers studied coalescence in a surfactant stabilized concentrated 2D emulsion where they found that one coalescence event can result in an avalanche of similar events destabilizing the entire assembly of drops[63].

In this chapter, we propose a conceptual framework to study the system-level behavior of such problems. In the previous chapters where we studied the self-organization of drops in 2D microchannels using an agent based approach, phenomenological models were proposed to explain drop-level interactions and the system-level behavior was simulated by considering the effect of all the drops together. However, not all the interactions are easy to model from a first principles approach. Bremond et al in their experiments realized that the sensitive dependence of coalescence on local conditions made the process appear stochastic. We make one of the first attempts to study such problems in droplet

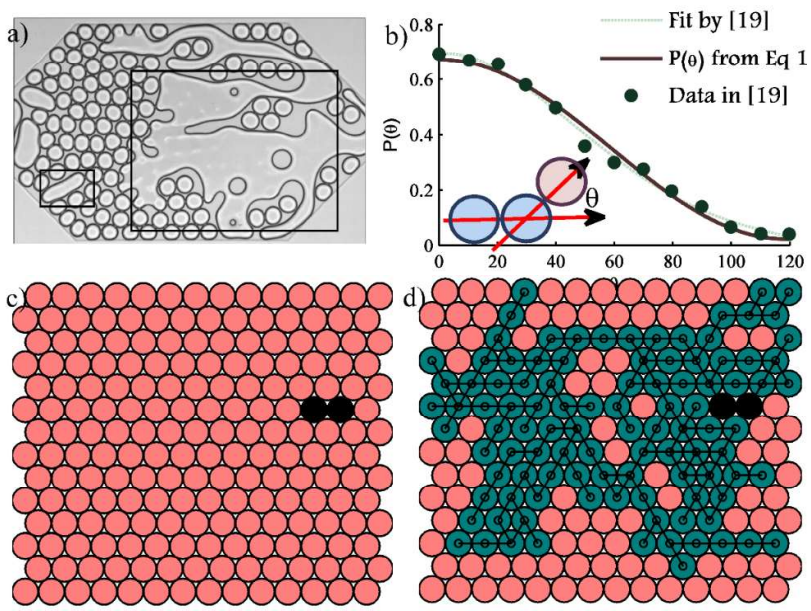

Figure 6-1 a) Experimental evidence of avalanches (snapshots) of different sizes (see inside box) (Bremond et al, 2011) [courtesy: Nicholas Bremond for sharing video results not available in literature]; b)Probability of coalescence as a function of theta (data digitized from[63]), fit- polynomial[63] and $P(\theta)$ according to Eq 6-1; c) A realization in the stochastic simulation that shows very little propagation, d) Realization showing high levels of propagation. [Black: initial pair that is made to coalesce; Green drops connected by yellow lines: drops that have coalesced; Peach: Free drops that are yet to coalesce] [videos enclosed in CD: different realizations of the process: small and large avalanches]

microfluidics through a stochastic agent based framework. In this chapter, we address the problem of coalescence propagation observed by Bremond and co-workers, where we try to understand coalescence propagation in 2D ensemble in a Hele-Shaw geometry. Drops can be packed tightly in such a microchannel to form a 2D concentrated emulsion. Stability of the emulsion depends on its immunity to coalescence events. If local coalescence events propagate through the assembly of drops, stability is compromised. Hence it is important to understand collective behavior of drops in 2D microchannels.

Drops coalesce when the thin film of continuous phase fluid between them drains and the drops meet. Experimental results show a rather counter-intuitive result where two closely placed drops coalesce upon decompression[8]. This is possible because when two drops are pulled apart, the low pressure between the drops deforms and pulls both the interfaces together facilitating contact, which results in coalescence. Efforts have been made to understand the mechanism of coalescence[65,66,88]. In a concentrated emulsion, when two drops coalesce they move towards each other. In the process they get pulled away from every other drop in the neighborhood. This retraction results in a low pressure region around the coalescing pair, which avalanches into a cascade of coalescence events[63]. In a 2D microchannel, during an avalanche, drops self-organize (re-arrangement, shape

relaxation[63]) inside the channel as they coalesce, making the problem complicated to model from a first principles approach. Also, the high sensitivity of coalescence propagation to factors like the film thickness and surfactant concentration and the continuous organization of drops and the shape relaxation of the growing cluster make the propagation appear seemingly stochastic. Hence not every coalescence event results in an avalanche. The boxed portions in Figure 6-1a show the different avalanche sizes observed in microchannels that were a result of two separate coalescence events. To understand this behavior, Bremond et al considered a combination of three drops and experimentally measured the probability $P(\theta)$ of drop 3 to coalesce with a coalescing pair (1 and 2) as a function of the orientation of the three drops (defined by θ) [63] (see Figure 6-1b, where the inset shows the angle θ that the drop 3 makes with the pair of drops 1 and 2). However, the function P does not shed light on the system level collective behavior, propagated coalescence, which is a multi-drop interaction phenomenon. Also from a scientific perspective it would be interesting to understand the effect of the microchannel design on the probability of a coalescence avalanche that can de-stabilize the whole assembly of drops (a typical destabilization is shown in the larger box in Figure 6-1a). In summary, we seek to answer the following questions regarding propagated coalescence: (i) how does one utilize the probability of local coalescence events, to study the system-level behavior, (ii) how is the stochastic nature of a coalescence event in a concentrated emulsion related to the destabilization of the drop assembly, and (iii) do microchannel design choices affect this coalescence propagation?

6.2 STOCHASTIC FRAMEWORK

We answer these questions through a stochastic bottom-up simulation framework that incorporates the measure of probability$P(\theta)$experimentally obtained by Bremond et al[63] to simulate the coalescence propagation in a 2D system that employs large number of drops. Bremond et al. fit a fourth order polynomial for the probability data. But a cosine functional form would explain the physics better. When two drops coalesce they move towards each other with a velocity$U_c(t)$. A third drop present in the neighborhoods which makes an angle θ with the coalescing pair, will experience a pulling effect $U_c(t)Cos\big(\theta(t)\big)$. We find that the experimentally measured P (Figure 6-1b) follows a trend similar to the above expression. In the dynamic coalescence process, as time proceeds, θ (except for the case where all three drops are positioned on a straight line) and

U_c decrease, with U_c decreasing exponentially[63]. Hence a more general functional form $ACos[B\theta] + C$, as shown in Eq 6-1 is able to explain the θ dependence of P, where $\{A, B, C\}$~$\{0.32, 1.57, 0.36\}$ for Bremond's data[63]. Further, we introduce a continuation parameter (while retaining the functional form) α to study a large spectrum of systems, from non-coalescing ($\alpha = 0$) to readily coalescing (large α). The parameter α will take a value of one for the case of Bremond's experiments.

$$G = ACos[B\theta] + C$$
$$P(\theta) = \begin{cases} 0 & \alpha G < 0 \\ \alpha G & 0 \leq \alpha G \leq 1 \\ 1 & \alpha G > 1 \end{cases} \quad \text{6-1}$$

Drops (represented as circles) can be assumed to be static because in typical microchannel flows, the average velocity of the drops $O(10^{-3})ms^{-1}$ is orders of magnitude smaller than the coalescence propagation velocity $O(10^{-1})ms^{-1}$ [63]. Hence, in our framework, propagation is studied on a lattice where the positions of drops are fixed. A cluster of drops is represented by circles connected by line segments. A randomly chosen pair of drops is allowed to coalesce. This triggers additional coalescence events with its neighbors based on experimentally measured P. The newly coalesced drops trigger similar coalescence events in their respective neighborhoods and the process continues till all the drops stop coalescing. In reality, growing clusters as shown in Figure 6-1a, Figure 6-2a, b contains local regions of high curvature, which result in dynamic rearrangement. Its effect on propagation, along with other sources of uncertainty that have to be accounted for in a complete numerical simulation has been implicitly captured in P. From Figure 6-2a, b (see boxed regions) it is also clear that one drop can coalesce with multiple drops during propagation. Hence the following algorithm is developed, considering all these factors, to study propagated coalescence.

6.2.1 Algorithm

I. A 2D hexagonal lattice with n^2 drops is initialized (with n rows and n columns; aspect ratio=1) (see Figure 6-1c, d),

II. Coalescence is initiated through a randomly chosen pair of drops i and j which are represented as circles with a black fill in Figure 6-1c and d,

III. Drops i and j are assigned to the set Ac (active drops) in the following manner $Ac = \{\{i, j\}, \{j, i\}\}$ where the first element of the ordered pair represents the node from

which the propagation is about to happen and the second element is used to determine the angle made by the pair with their neighboring drop.

IV. A neighbor set Nc is generated which is represented as $Nc = \left\{\left\{n_{i,j}^1, n_{i,j}^2, .. n_{i,j}^p\right\}, \left\{n_{j,i}^1, n_{j,i}^2, .. n_{j,i}^q\right\}\right\}; p, q \leq 5$, a set of n-tuples where n can take a maximum of 5. Each list of n-tuples corresponds to a specific ordered pair in Ac. Definition of neighbor: drop 1 is the neighbor of drop 2 if the distance between them in the lattice is equal to the sum of the radii of the drops 1 and 2.

V. If $Nc \neq \emptyset$ continue; else set $Ac \neq \emptyset$ and go to step VII

VI. Coalescence propagation through each of the elements (drops) of the set Nc is effected stochastically using the probability $P(\theta)$,

   a. choose a drop (k) from the set Nc
   b. compute the probability based on its orientation with the corresponding ordered pair in set Ac
   c. select a uniform random number $Uc \in (0,1]$
   d. if $U \leq P(\theta_k)$ then k has coalesced with the cluster – add this drop to a new set Ac_{new}
   e. repeat the steps for all drops in all the n-tuples in the set Nc

VII. Set $Ac = \emptyset$ and assign $Ac = Ac_{new}$; if $Ac \neq \emptyset$ go to step III else continue

VIII. Terminate

A randomly chosen coalescing pair of drops has ten neighbors (if the pair is not at an edge of the lattice). Propagation can happen through all these neighbors. But the stochastic nature of the problem reduces the chances of propagation through all neighbors based on $P(\theta)$. The framework that we propose, as explained in the algorithm, effectively uses $P(\theta)$that explains coalescence locally to simulate propagation in the entire assembly.

6.3 PROPAGATION DYNAMICS

6.3.1 Nature of propagation

The proposed algorithm is event based. Simulations using this algorithm start with a coalescence of a random pair, which we call the first generation or the first event. Propagation through the neighbors of the coalesced pair leads to the second event and so on. Because the simulations are stochastic, every realization will yield a different result. Results from simulations presented in Figure 6-1c and d indicate that the stochastic

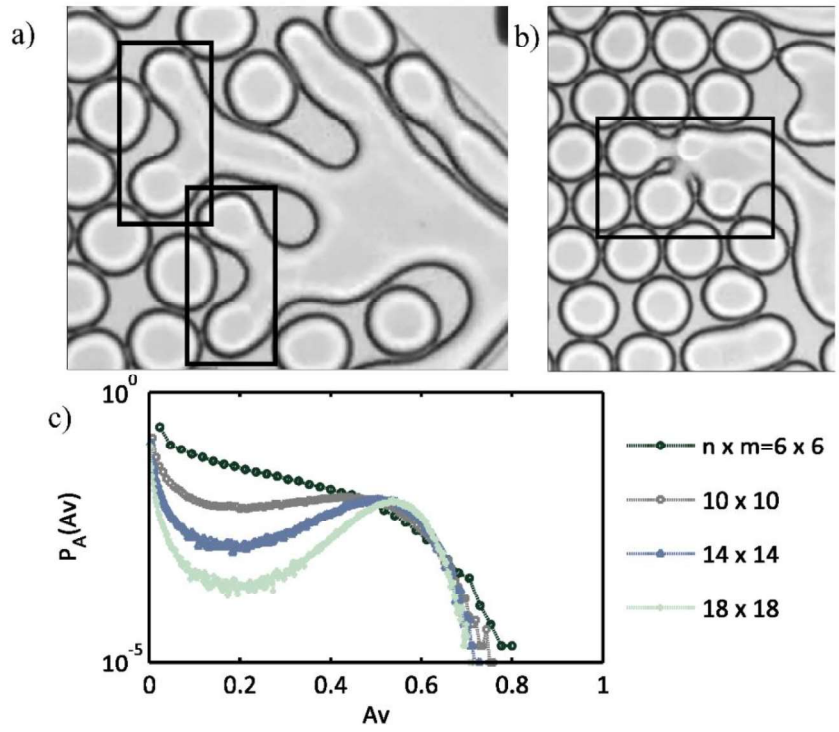

Figure 6-2 a), b) Evidence for propagation through multiple drops and formation of complex shapes that have local regions with high curvature [courtesy: Nicholas Bremond for sharing video results not available in literature] c) Probability of occurrence of an avalanche $P_A(Av)$ as a function of the size Av (normalized with $Av_{max} = 3nm - 2(n+m) + 1$ where the lattice is of size $n \times m$,) of the avalanche for different system sizes ($n \times m$). 10^5 independent simulations were carried out to generate this probability curve.

framework is able to capture propagation events with avalanches of different sizes, where size of the avalanche is the number of individual coalescence events in an avalanche. While this demonstrates the ability of the proposed approach to capture the physics as seen in the experiments, one would like to understand more quantitatively, the probability with which an avalanche of a certain size is likely to occur. To probe this we carry out $>10^5$ independent simulations to understand the ensemble behavior of the system. This analysis is carried out for different system sizes. From the ensemble data, the probability of avalanche P_A is computed as a function of size of the avalanche and is plotted in Figure 6-2c for different system sizes considered. For a given $P(\theta); \alpha = 1$, systems with $n \leq 7$ (49 drops) have a $P_A(Av)$ curve that decreases monotonically with increasing avalanche size. Interestingly, larger systems where n>7 show emergent behavior. In such cases, the $P_A(Av)$ curve becomes non-monotonic and larger avalanches occur with greater probability than smaller ones (a new peak emerges). This is a very interesting, difficult to comprehend emergent characteristic that is of critical practical importance from a stability view point because probability of avalanches is directly related to the probability of

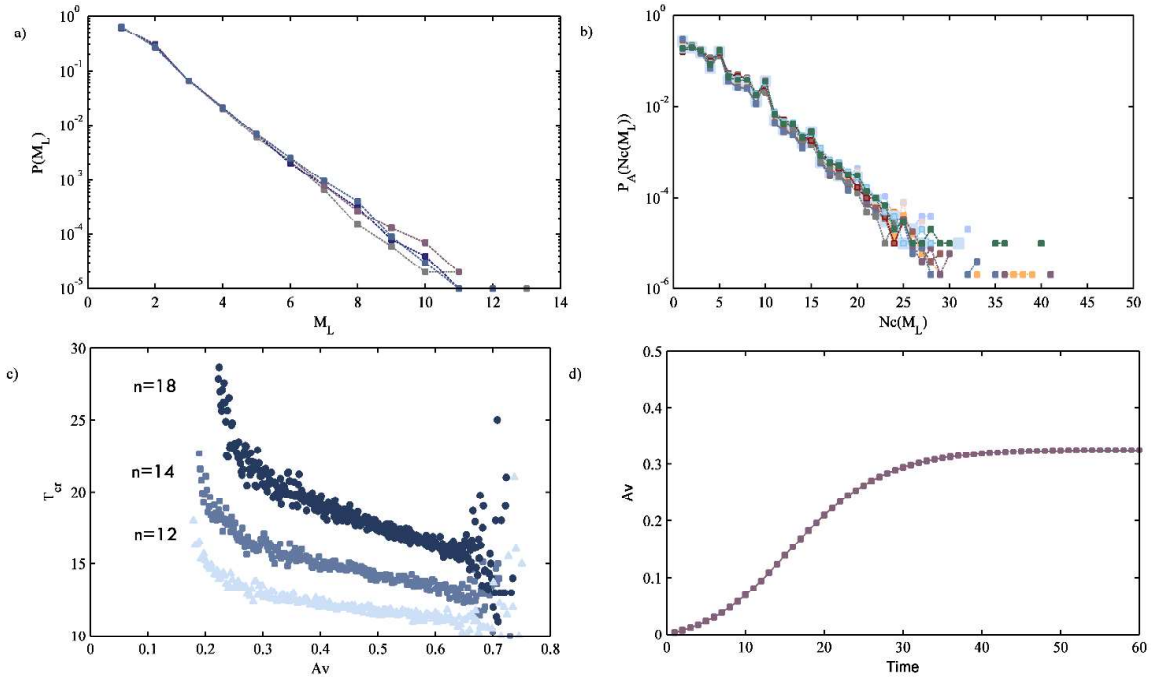

Figure 6-3 a) Probability of finding M_L active drops in last generation ($P(M_L)$) as a function of the size (M_L) for systems with n ranging from 6-22; b) Probability of finding $Nc(M_L)$ neighbors [$P(Nc(M_L))$] of active drops in last generation as a function of the size ($Nc(M_L)$) for systems with n ranging from 6-22; c) Average number of events or generations (T_{cr}) taken by a growing avalanche to reach the size with the minimum probability; d) Time (in generations) evolution of an avalanche size (Av) averaged over $\sim 10^5$ simulations. A sigmoidal growth curve is seen which is characteristic of an autocatalytic process

destabilization of the drop assembly. As the system size increases, the region near the minima of the $P_A(Av)$curve becomes lesser than 10^{-5} and the maxima (peak) sharpens, which suggests that an experimentalist working with $O(10^3)$ drops, for this system as characterized by $P(\theta)$, would observe either very small avalanches or large ones that cover almost the whole channel. It is worth reiterating here that such non-intuitive insights about the multi-drop system are being derived from purely a 3-body probability function and a stochastic framework. The next step is to understand the reasons behind the propagation dynamics showing critical behavior.

In an attempt to understand the appearance of the hump in the $P_A(Av)$, we try to investigate why certain avalanches in the size range $\sim 0.1 - 0.3$ have a lower probability of occurrence. To do so, we observe the average ensemble behavior at the last generation and the dynamics near the avalanche size that has the minimum probability. As coalescence propagates through a sequence of events, the size of Ac varies. In the last generation (event) there are M_L drops in the set Ac, which have to stop coalescing for propagation to cease. From Figure 6-3a, it can be seen that it is highly likely that a small M_L will be found. From Figure 6-3b it is also evident that the probability of finding enough neighbors in the

last generation follows a similar trend. So for a typical avalanche, the active drops have to reduce to a small number before the propagation stops. Av_{min} is the point at which $P_A(Av)$ shows a minimum in Figure 6-2c. From the dynamics of the avalanche process, we compute the average number of events (number of generations) taken for a growing avalanche to reach (or cross) the size (Av_{min}) with minimum probability. From Figure 6-3c one can infer that avalanches that stopped growing when its size was close to the minima (Av_{min}) take longer time to reach Av_{min} than the larger avalanches that have higher probability of occurrence. This means that the rate of cluster growth of an avalanche when its size is Av_{min} is higher for avalanches with higher probability of occurrence. Along with the fact that most of the clusters stop propagating only when M_L is small, the computed results suggest that for an actively growing cluster to stop propagating the number of active drops should reduce, which makes this event less likely. This helps us understand why avalanches of a certain size range have lower probabilities of occurrence.

Hence, one can conclude that if a cluster does not stop propagating when its size is small, it is likely to grow to cover almost the whole system (see Figure 6-1a, d). It is important that we understand the reason for this 'runaway' like behavior. We propose that as the cluster grows, the size of Ac increases, which in turn amplifies the rate of cluster growth making coalescence propagation autocatalytic. A plot of the average avalanche size as a function of the number of events (Figure 6-3d) shows the sigmoidal nature of the growth which is a characteristic of an autocatalytic process. For example, Rittaco and co-workers also observed a sigmoidal like death curve when investigating lifetime of bubble rafts[141]. The authors use an algorithm where there is multi-drop interaction and report $P_A(Av)$with features similar to ours. However, they attribute their observation to the cooperative nature of the process where the death of a bubble influences the probability of the death of its neighbors. But in our simulations the drops do not show cooperative behavior- because the probability of propagation is a function only of the orientation of drops- yet they show a hump in the $P_A(Av)$plot and a sigmoidal growth curve. As a result, we hypothesize that the sigmoidal like behavior can only be a result of the autocatalytic nature of the propagation.

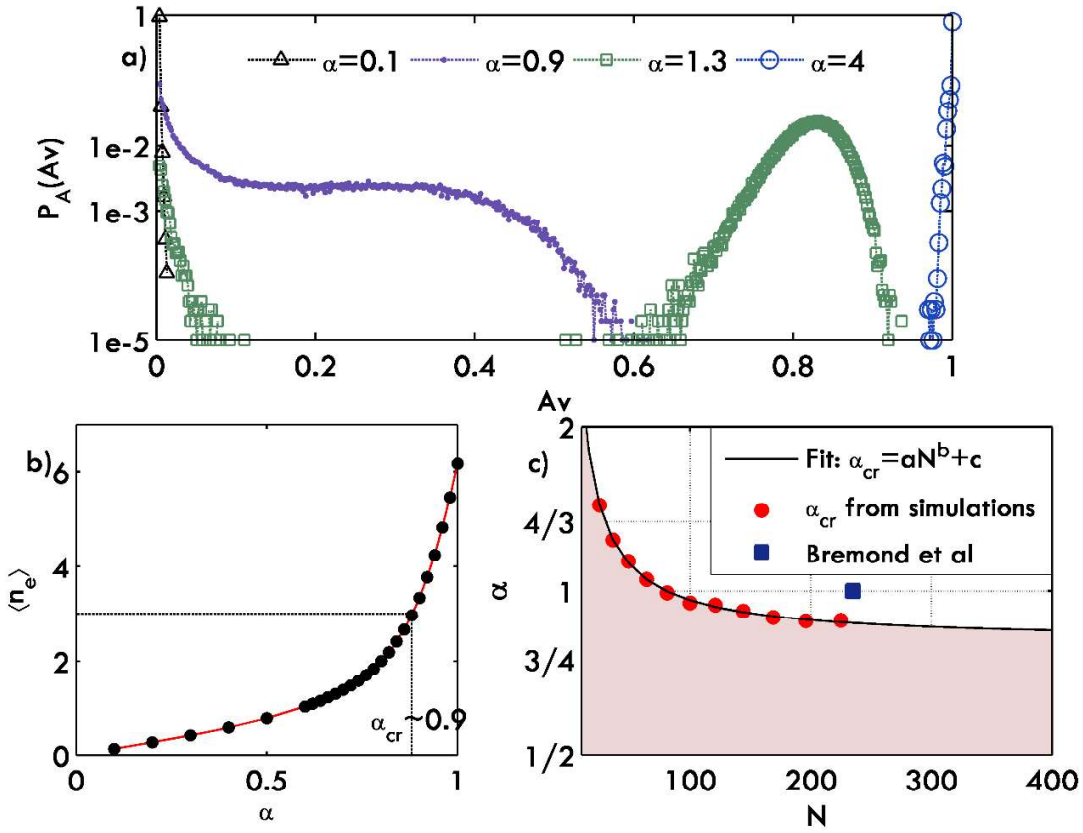

Figure 6-4 a) Probability of avalanche $P(Av)$ as a function of size (Av) for different probability measures $P' = \alpha P; \alpha \geq 0$; b) The weighted sum of neighbors $\langle n_e \rangle$ as a function of α; at $\alpha_{cr} \sim 0.9$; $\langle n_e \rangle = 3$; System size=196 drops; c) Parametric plot: Critical value of α plotted as a function of N (total drops which is equal to n^2); Shaded region- no autocatalytic behavior and vice versa

6.3.2 Reason for autocatalytic behavior

Several important questions arise at this juncture: Why is coalescence propagation autocatalytic? Further, does a fluid system as the one studied here always show autocatalytic behavior? To answer these questions, we need to analyze the two important features of coalescence, the propagation mechanism, which depends on the number of neighbors available for propagation and the probability $P(\theta)$ which captures the intrinsic tendency for coalescence for different fluid systems.

In an effort to understand the autocatalytic nature of the propagation, we study the number of neighbors available for coalescence using a simple conceptual measure that captures the nature of propagation. It is evident that during propagation each active drop has a certain number of neighbors $_i$ with which it can coalesce. Based on this, one could calculate an average number of drops around an active drop. However, this measure might not be very illuminating as the probabilistic nature of the propagation and the θ dependence of the

probability does not favor coalescence through all the neighbors equally. Hence, we find the effective number of neighbors (n_e) available for coalescence by carrying out a weighted sum of the neighbors $n_e = \sum_i P(\theta_i) n_i$, where the weights are the associated propagation probabilities for the corresponding neighbors. We then use the idea of "number averaging" to find the average effective number of neighbors $\langle n_e \rangle$ averaged over time and all possible realizations which is given by the expression $\langle n_e \rangle = \left({}^{1}/_{EN}\right)\left(\sum_{1}^{EN}\left(\left(1/T_f\right)\sum_{t=1}^{T_f} n_e\right)\right); EN \sim O(10^5)$. Remarkably, we find that the critical value where the transition to dominant autocatalytic behavior occurs is at $\langle n_e \rangle \approx 3$. This is a result that is quite non-obvious.

6.4 EFFECT OF PROBABILITY

When the fluids or the surfactant concentration in the microchannel system are changed, the propensity to coalesce is captured by the changes in $P(\theta)$. To capture the effect of this change, we carry out simulations by varying the continuation parameter α. As one would expect, for the asymptotic cases of α being zero $P(\theta)$=0 and very large $P(\theta) = 1$, the behavior is deterministic: no propagation and complete propagation respectively. Figure 6-4a shows the $P_{Av}(Av)$ plot for different values of α. For values of $0 < \alpha < \alpha_{cr}$, (in this case $n = 14$ where$\alpha_{cr} = 0.88$, corresponding to $\langle n_e \rangle = 3$) the probability of avalanche decreases monotonically with size, showing no autocatalytic behavior. Propagation becomes dominantly autocatalytic as $\alpha_{cr} > 0.88$ and the hump starts to appear. The most prominent feature of this non-monotonic region is the presence of two most favorable outcomes, no propagation and autocatalytic propagation resulting in large avalanches (corresponds to the maxima in the Figure 6-2c, Figure 6-4a). For very large α, we see a monotonically increasing trend as seen in Figure 6-4a. To evaluate the behavior across the complete spectrum we observe the evolution of $\langle n_e \rangle$ as α increases.

Figure 6-4b shows how $\langle n_e \rangle$ varies with α. The α corresponding to $\langle n_e \rangle = 3$ marks the critical transition to dominantly auto-catalytic behavior. To understand the effect of system size on autocatalytic behavior, this numerical exercise is repeated for different values of N and the corresponding α_{cr} is computed. Figure 6-4c shows the plot between α_{cr} and N which divides the parameter space into two regions: in the shaded region a system would not show auto-catalytic behavior and vice versa. In Bremond's work $N \cong 235$ and $\alpha = 1$,

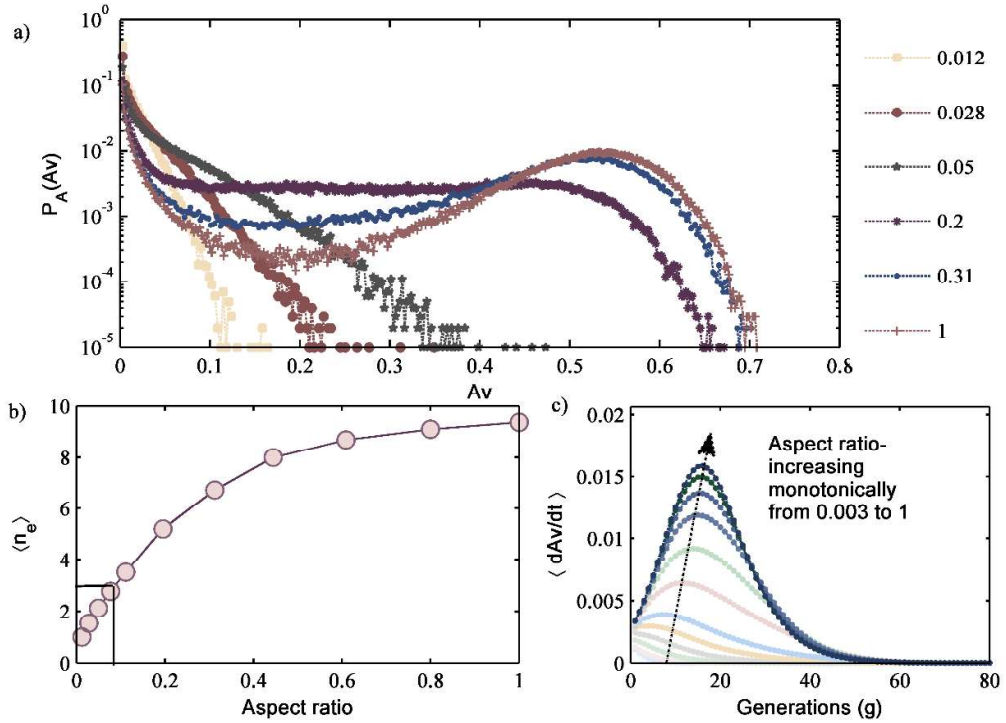

Figure 6-5 a) Probability of occurrence of an avalanche as a function of the size Av (normalized with Av_{max}) of the avalanche for different aspect ratios of the drop assembly (total number of drops=324 drops); b) The weighted sum of neighbors $\langle n_e \rangle$ as a function of aspect ratio (0.003 to 1); at aspect ratio~0.1, $\langle n_e \rangle = 3$; c) Average avalanche growth rate as a function of time in generations for different aspect ratios (arrow indicates the the trend of the plot for monotonically increasing aspect ratios)

we find that this point lies in the autocatalytic region in Figure 6-4c (marked by a blue square), confirmed by the experiments reported in that paper.

6.5 EFFECT OF PACKING

With our stochastic formulation we are able to answer two important scientific questions: 1) for a given fluid system what is the drop ensemble size before autocatalytic propagation dominates and destabilizes the system? 2) When the number of drops is fixed and for a given fluid system, can the drops be packed in different ways that would reduce autocatalytic propagation? From Figure 6-4c, for a given fluid system as characterized by a constant α, one can identify the critical number of drops that can be packed together before the propagation of coalescence in the ensemble becomes autocatalytic. Quite amazingly, our simulations show that fluid systems whose $\alpha <$ ◄can form stable emulsions largely independent of size: propagation steps are non-autocatalytic, which would allow for a very large stable assembly of drops in channels with aspect ratio equal to1. Qualitatively similar transitions have been observed in the experiments of Baret and co-workers: when the effective surfactant concentration on the drop-continuous phase

interface increases there is a sharp transition from unstable to stable emulsions[139]. Further, for the case where we have a constant number of drops for a certain fluid system, we study the effect of aspect ratio of the drop-assembly on its stability.

Our simulations show that as the aspect ratio deviates from the value one, there is a reduction in the propagation which results in the disappearance of the hump as seen in Figure 6-5a. Though the hump disappears for an aspect ratio value of 0.2, propagation remains autocatalytic and the average weighted neighbors available (see Figure 6-5b) is greater than 3 (confirmed by the non-monotonic curves in Figure 6-5c; a non-monotonic curve represents sigmoidal growth of an Avalanche). Another very interesting and non-intuitive result is that the presence of a hump implies autocatalytic propagation but the absence of the hump does not imply absence of autocatalytic propagation. Nonetheless, changing the aspect ratio affects the propagation because a cluster grows in all directions and presence of a wall would hinder the growth in that direction (edge of the assembly in our case) reducing the average cluster size. We find that when the aspect ratio is less than 0.1, the propagation is no longer autocatalytic. This suggests that as the channel designs force the coalescence front to move increasingly in one dimension, autocatalytic propagation becomes less likely.

6.6 CONCLUSION

A stochastic agent-based framework has been developed to study coalescence propagation in microchannels that employ a concentrated 2D emulsion. Here the agents are the drops which are fixed on a lattice. The interaction between the drops is characterized by the probability data $P(\theta)$- experimentally measured by Bremond et al[63]- which explains the probability with which drops will coalesce locally - to study the system level propagation. The stochastic simulations capture the inherent autocatalytic nature of the propagation process for large system size (N). This nature of propagation results in two likely scenarios: one where propagation is almost absent and the other where propagation can lead to destabilization of almost the entire drop assembly. This is in accordance with the observations of Bremond et al in their experiments. It is interesting to see how a simple conceptual framework- that does not explicitly account for drop motion and anisotropic drop-packing in a microchannel- captures the avalanching process that leads to destabilization of the assembly. We follow a simple weighted averaging procedure to compute the effective number of neighbors available for coalescence. We infer that the

propagation is dominantly autocatalytic only if the average effective neighbors available for coalescence is greater than three. We find that a cosine functional form for the $P(\theta)$ based on the mechanism of propagation which involves decompressing of drops, fits the data well. This suggests that the mechanism of the process has manifested itself in the probability data. The effect of fluid properties on the probability is captured by a continuation parameter α. We find that the propagation is autocatalytic only after a critical α across which there is a sharp transition from stable to unstable behavior. Also, for a given fluid system (constant α) we can estimate the critical size of the system beyond which the propagation will be autocatalytic. Understanding the propagation phenomenon can help in the design of microchannels. We find that aspect ratio of the assembly of drops has an impact on propagation dynamics: aspect ratio far from unity reduces the average avalanche size thereby increasing the stability.